

COGNITIVE NEUROSCIENCE

Automatic representation of a visual stimulus relative to a background in the right precuneus

Motoaki Uchimura,^{1,2,3} Tamami Nakano,^{1,2,4} Yusuke Morito,⁴ Hiroshi Ando^{4,5} and Shigeru Kitazawa^{1,2,4}¹Dynamic Brain Network Laboratory, Graduate School of Frontier Biosciences, Osaka University, 1-3 Yamadaoka, Suita, Osaka 565-0871, Japan²Department of Brain Physiology, Graduate School of Medicine, Osaka University, 1-3 Yamadaoka, Suita, Osaka 565-0871, Japan³Japan Society for the Promotion of Science, 5-3-1 Kojimachi, Chiyoda, Tokyo 102-0083, Japan⁴Center for Information and Neural Networks (CiNet), National Institute of Information and Communications Technology, Osaka University, Suita, Osaka 565-0871, Japan⁵Multisensory Cognition and Computation Laboratory, National Institute of Information and Communications Technology, 3-5 Hikaridai, Seika, Kyoto 619-0289, Japan**Keywords:** adaptation, background, egocentric, fMRI, precuneus

Abstract

Our brains represent the position of a visual stimulus egocentrically, in either retinal or craniotopic coordinates. In addition, recent behavioral studies have shown that the stimulus position is automatically represented allocentrically relative to a large frame in the background. Here, we investigated neural correlates of the 'background coordinate' using an fMRI adaptation technique. A red dot was presented at different locations on a screen, in combination with a rectangular frame that was also presented at different locations, while the participants looked at a fixation cross. When the red dot was presented repeatedly at the same location relative to the rectangular frame, the fMRI signals significantly decreased in the right precuneus. No adaptation was observed after repeated presentations relative to a small, but salient, landmark. These results suggest that the background coordinate is implemented in the right precuneus.

Introduction

Our brains represent a position of a visual stimulus (or a target) relative to our body parts, such as the eyes and the head (Galletti *et al.*, 1993; Sereno *et al.*, 1995; Duhamel *et al.*, 1997; Sereno & Huang, 2006; d'Avossa *et al.*, 2007; McKyton & Zohary, 2007; Crespi *et al.*, 2011). A target position can also be represented in relation to objects or landmarks that do not belong to us. An allocentric representation is used for intentionally memorising a target position for the subsequent execution of memory-guided movement (Karn *et al.*, 1997; Sheth & Shimojo, 2004; Obhi & Goodale, 2005; Byrne *et al.*, 2010). In marked contrast, recent studies in psychophysics have shown that the brain instantly (within a fraction of a second) and automatically (without any conscious intention) represents a stimulus position relative to a 'frame' in the background of a scene, even when the stimulus position relative to the frame has no relevance to the ongoing task (Boi *et al.*, 2011; Lin & He, 2012; Uchimura & Kitazawa, 2013). This automatic process did not occur when a large frame was replaced with a small rectangle (Uchimura & Kitazawa, 2013). These results suggest that the background coordinate for

automatically representing a visual stimulus is distinct from the one for memorising a target position for an endeavor.

Previous studies that used monkeys have demonstrated that neurons in the supplementary eye field (SEF) and parietal area 7a are involved in the intentional process of memorising a target relative to a line or a letter-like object (Olson & Gettner, 1995; Chafee *et al.*, 2007). A recent human imaging study also suggested that endogenous attention, in terms of an object-centered coordinate, involves the SEF and the superior parietal lobe (Szczepanski *et al.*, 2013). In contrast, little is known regarding the neural mechanisms of the automatic process for representing a visual stimulus in terms of the background coordinate.

To elucidate the neural correlates of the background coordinate for an automatic stimulus representation, we used an fMRI adaptation technique (Grill-Spector *et al.*, 2006; Bernier & Grafton, 2010; Van Pelt *et al.*, 2010). In the first experiment, we identified the brain regions that showed a decreased response when a visual stimulus was repeatedly presented at the same location in terms of a large rectangular frame (Fig. 1). In the second experiment, we replaced the large frame in the first experiment with a small, but salient, rectangular landmark (Fig. 3A). We expected that little adaptation would be observed with the small landmark because we previously found that automatic encoding did not occur with a small but salient square (Uchimura & Kitazawa, 2013).

Correspondence: S. Kitazawa, ¹Dynamic Brain Network Laboratory, as above.
E-mail: kitazawa@fbs.osaka-u.ac.jp.

Received 24 February 2015, revised 23 April 2015, accepted 27 April 2015

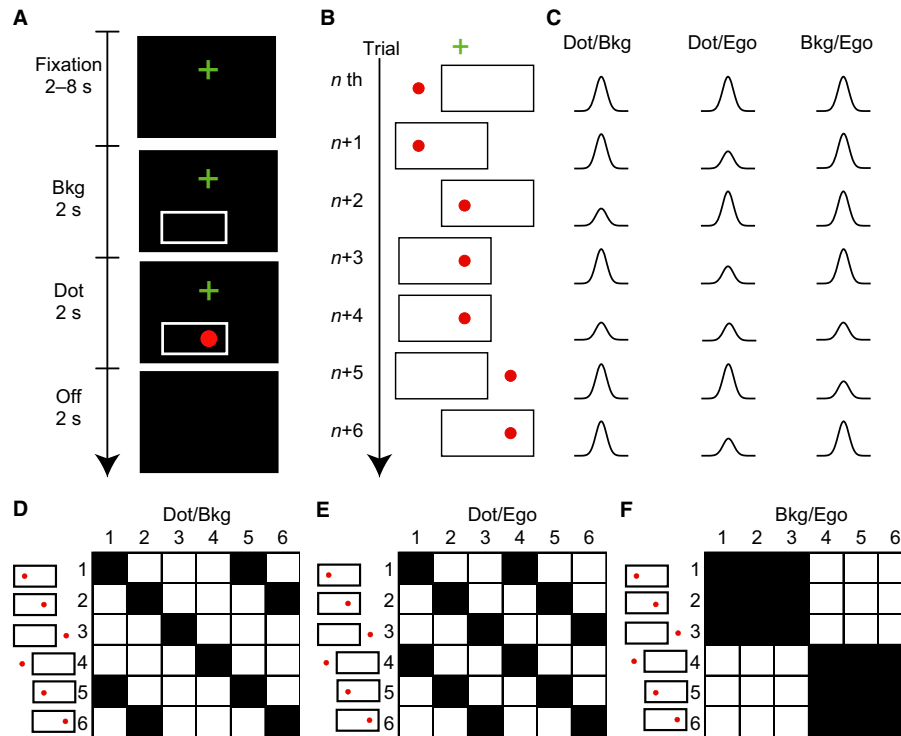


FIG. 1. Study designs based on fMRI adaptation. (A) A sequence of visual stimuli in one trial in Experiment 1. A trial was initiated by the presentation of a cross for fixation (Fixation, 2–8 s), followed by the presentation of a background frame (Bkg; 2 s) and then a visual stimulus for 2 s (Dot). The participants had to judge whether the stimulus was an apple or a red dot and respond by pushing a button if it was an apple. Following a blank period (Off; 2 s), the next trial was initiated. (B) Examples of visual stimuli in seven successive trials [n th to $(n + 6)$ th]. Note that the dot appeared at three locations (left, middle and right) and the frame appeared at two locations (left and right). Thus, there were six patterns of visual stimuli. (C) Hypothetical decreases in BOLD signal responses as a result of adaptation. Changes are shown separately for areas where the dot position is represented in terms of the background frame (Dot/Bkg; left column), the dot in the egocentric (eye- and head-centered) coordinates (Dot/Ego; middle) and the background in terms of the egocentric coordinates (Bkg/Ego; right). For example, a dot was presented at the same location relative to the background frame in both $(n + 1)$ th and $(n + 2)$ th trials. The response in the $(n + 2)$ th trial should be smaller in amplitude due to adaptation in areas where the dot was represented in terms of the background. Another decrease was expected in the $(n + 4)$ th trial. Similarly, a smaller response was expected in a trial in which a dot (or a background frame) was presented in the same position as in the previous trial in terms of the designated coordinate. (D–F) Six-by-six binary repetition matrices that show a repetition (1, black) and a novelty (0, white) in the dot (or background) position from one trial to the next trial in terms of the designated coordinate: each row represents one of six visual stimuli in one trial, and each column represents one of six in the next trial. A dot was presented at the same location in terms of the background frame coordinate in 10 of the 36 combinations (black cells, D) and in terms of the egocentric coordinates in 12 of the 36 combinations (E). A background frame was presented at the same location in terms of the egocentric coordinates in 18 of the 36 combinations (F).

Material and methods

Participants

Thirty-four healthy young adults (25 male, nine female, ranging in age from 20 to 31 years) participated in either Experiment 1 ($n = 16$), Experiment 2 ($n = 16$), or both ($n = 2$). Thus, 18 participants were included in each of the Experiments 1 and 2. All participants had normal or corrected-to-normal vision, with no history of neurological disorders. They were all right-handed (laterality quotient, +70 to +100) according to the Edinburgh Inventory (Oldfield, 1971). All except for one of the co-authors (M.U.) were naive to the purpose of the experiments. Written informed consent was obtained from all participants prior to the experiments. This study was approved by the Ethical Review Board of Osaka University, Graduate School of Frontier Biosciences. The study conforms with World Medical Association Declaration of Helsinki.

Task

Each participant lay supine on a table in an MR scanner with the head stabilised by urethane foam pads. The participant viewed a screen ($17^\circ \times 13^\circ$), fixed at the back of the magnet’s bore, through

a mirror placed above a head coil. Each participant was instructed beforehand to fixate on a cross ($0.5^\circ \times 0.5^\circ$) when it was presented on the screen (Fig. 1A, Fixation), ignore a rectangular frame ($8^\circ \times 4^\circ$) that was presented with a delay randomly chosen from 2, 4, 6 or 8 s [Background (Bkg)], and judge whether a visual stimulus was a red dot or a red apple (0.4° in radius) when the visual stimulus was presented 2 s later for 2 s (Dot). When the stimulus was an apple, the participants were required to respond by pushing a button held in the right hand. The next trial was initiated after a blank of 2 s (Off).

In Experiment 1, the cross was always presented 1.5° above the center of a dark screen (Fig. 1A). The rectangular frame was positioned at one of two locations, with its center 2° to the right or 2° to the left, and 3.7° below, the fixation point. The visual stimulus was presented at one of three locations: -4° , 0° or $+4^\circ$ to the right of the screen center at a horizontal level of 3.7° below the fixation point. As a result, there were six patterns of visual stimuli (two frame positions \times three dot positions; Fig. 1B). Each run of Experiment 1 consisted of 37 trials, which included all 36 permutations in two successive trials (six patterns \times six patterns; Fig. 1D–F). The order of the 36 permutations was randomly chosen for each run. In each run, the dot was presented at the same location 10 times in

terms of the background frame coordinate (filled squares; Fig. 1D) and 12 times in terms of the egocentric coordinates (Fig. 1E). The background frame was presented at the same location 18 times in terms of the egocentric coordinates (Fig. 1F). An apple was presented in two trials for each run, which were chosen randomly from 26 trials in which the position of the visual stimulus was not repeated in terms of the background frame coordinate. Each participant experienced 10 trials for familiarisation and participated in six runs of 37 trials. Each run lasted ~ 404 s.

In Experiment 2, the size of the rectangular frame was reduced to $0.9^\circ \times 0.5^\circ$ to ensure that the area subtended by the frame matched the area of the red dot (Fig. 3A). The experimental conditions were otherwise identical to the conditions in Experiment 1. That is, the small rectangular frame ($0.9^\circ \times 0.5^\circ$) was positioned at one of two locations, with its center 2° to the right or 2° to the left, and 3.7° below, the fixation point. The visual stimulus (0.4° in radius) was presented at one of three locations: -4° , 0° or $+4^\circ$ to the right of the screen center at a horizontal level of 3.7° below the fixation point. Thus, the distance between the centers of the frame and the test visual stimulus was -6° , -2° , $+2^\circ$ or $+6^\circ$, and the frame and the test never overlapped spatially. They were presented together for 2 s during the entire period of the dot presentation (Fig. 3A).

The participants seldom made errors in the deviant detection (Table 1). The rate of missing an apple (false negative) was 0/12 in the majority of the participants (18/18 and 16/18 participants in Experiments 1 and 2, respectively), with a maximum rate of 2/12 (one participant in Experiment 2). The rate of false positives was 0/210 in the majority of the participants (15/18 and 14/18 participants in Experiments 1 and 2, respectively), with a maximum rate of 4/210 (one participant in Experiment 2).

Localiser experiments

Representing a target relative to the background is a part of visual function, but the system must also be at work when we manipulate a target in space. We thus conducted two experiments to localise neural correlates of the background coordinate relative to the visual and motor regions in general. In a visual localiser experiment, one of three annular black-and-white checkerboard patterns ($0-3^\circ$, $3-6^\circ$ or $6-12^\circ$ in radius) was flickered at 4 Hz (Serenio *et al.*, 1995), while the participants fixated on the center point of each annulus. One scan lasted 375 s; following an initial blank period of 15 s, each visual stimulus was presented for 15 s in series (45 s); the sequence of 15 + 45 s was repeated six times and followed by a final blank period of 15 s. Two scans were conducted for each participant.

The participants in Experiment 1 also participated in a motor localisation experiment. Each participant made sequential opponent finger movements by touching the tip of the thumb with the fingers

of the right or left hand in the order 5-3-4-2-5-3-4-2-5-3-4-2 (Kansaku *et al.*, 2005). Each run consisted of six 40-s epochs, in each of which a red or a blue square was presented on the screen to make the participants prepare for the movement with the right hand (blue square) or with the left hand (red). Then the square disappeared after a randomised period (9–19 s) to instruct the participants to start the prepared movement. The cues were presented in a fixed order for the color (blue, blue, red, red, blue, red) and duration (9, 19, 13, 11, 17, 15 s).

Data acquisition

Structural images for each participant were collected using a T1-weighted 3-D MP-RAGE sequence on a Siemens 3-Tesla whole-body scanner [repetition time (TR) = 2 s, echo time (TE) = 4.38 ms, flip angle = 80° , field of view 192×256 mm, resolution $1 \times 1 \times 1$ mm]. Functional images were collected using a gradient echo, echo-planar sequence (TR, 2.0 s; TE, 30 ms; flip angle, 80° ; isotropic nominal resolution, 3 mm; 34 adjacent contiguous slices with a 0.4-mm gap, thickness 3.4 mm). The slice positions were adjusted to cover the entire prefrontal, parietal and temporal cortices. Each participant completed six runs (216 scans per run). Each run was conducted for 431 s, which included an initial fixation period of 15 s followed by a 2-s blank period, 404 s during the task (37 trials), and a 10-s blank period at the end. The first four images of each run were discarded. During scanning, the gaze positions (eye movements) and pupil sizes were monitored and recorded continuously using an infrared video eye-monitoring system with a sampling rate of 240 Hz (NAC Image Technology, Tokyo, Japan). The eye blinks were detected and removed by analysing the pupil sizes as previously described (Nakano *et al.*, 2013). Each saccade was then automatically detected with a velocity threshold of $60^\circ/\text{s}$ and an acceleration threshold of $8000^\circ/\text{s}^2$ during the period of frame presentation (2 s) and dot presentation (2 s). The threshold velocity roughly corresponded to the peak velocity of a saccade with an amplitude of $1-2^\circ$ (Baloh *et al.*, 1975; Martinez-Conde *et al.*, 2009). The existence of a saccade with an amplitude $> 2^\circ$ was subsequently confirmed by the experimenter one by one for each detected trial. Regarding the 'frame coordinate,' we did not have to exclude trials with a saccade in theory because the frame coordinate must operate irrespective of whether the eyes moved. However, we removed the trials with a saccade above the aforementioned thresholds from subsequent analysis (1.4% of the total trials; 1.7% in Experiment 1 and 1.1% in Experiment 2). We further confirmed that the peak coordinates of major clusters that represented the background coordinate remained generally unchanged, regardless of whether we discarded the saccade trials.

Data analysis

We used SPM8 (Wellcome Trust Centre for Neuroimaging) for data preprocessing [slice timing, realignment for head motion correction, normalisation to the standard brain template (Montréal Neurological Institute template), resampling with a voxel size of $2 \times 2 \times 2$ mm³, and smoothing with a 4-mm (Experiments 1 and 2), or 8-mm (localiser experiments) full-width half-maximum Gaussian filter] and statistical analyses based on voxelwise signal changes. The 4-mm Gaussian filter was chosen to achieve a spatial resolution as small as 2-3 mm (Blankenburg *et al.*, 2003; Weibull *et al.*, 2008). A general linear model with the standard hemodynamic function of SPM (first level) and random effects analysis (second level) was used, after excluding the data from trials with the apple stimulus. In

TABLE 1. The number of errors in the deviant-detection task

	0/12	0/12	0/12	1/12	2/12
False negatives	0/12	0/12	0/12	1/12	2/12
False positives	0/210	1/210	2/210	3/210	0/210
d'	∞	∞	∞	3.57	∞
No. of errors					
Exp 1 ($n = 18$)	15	3	0	0	0
Exp 2 ($n = 18$)	13	1	2	1	1
Total	28	4	2	1	1

There were no false negatives in 34/36 participants, and no false positives in 29/36 participants. The d' is defined as $d' = -Z(\text{false negative rate}) - Z(\text{false positive rate})$, where the function $Z(p)$ is the inverse of the cumulative Gaussian distribution function.

the first-level analysis in Experiment 1, four regressors were defined [novel/repeated in terms of the background coordinate \times novel/repeated in terms of the egocentric (eye- and head-centered; Ego) coordinates: (i) novel Dot/Bkg and novel Dot/Ego; (ii) novel Dot/Bkg and repeated Dot/Ego; (iii) repeated Dot/Bkg and novel Dot/Ego; and (iv) repeated Dot/Bkg and repeated Dot/Ego] to examine adaptation to allocentric coding of the stimulus relative to the background (Dot/Bkg; Fig. 1D) and adaptation to egocentric coding of the stimulus relative to the self (Dot/Ego; Fig. 1E). The linear model was fitted to the fMRI time series for each voxel for each participant. Using the estimated parameters for each voxel, two null hypotheses (novel < repeated/Bkg; novel < repeated/Ego) were tested, and the resulting two sets of voxel values (*t*-statistic) for each comparison was subjected to the second-level analysis. Two regressors (novel/repeated in terms of the egocentric coordinates) were also defined to examine adaptation as a result of the repeated presentation of the background frame in terms of the egocentric coordinates (Bkg/Ego). Appropriate regressors and null hypotheses were also defined for Experiment 2 (Dot/Landmark, Dot/Ego, Landmark/Ego) and the localiser experiments.

In the second-level analysis, a *t*-test was used to determine whether the mean of 18 *t*-statistics was significantly greater than zero. For data analysis in Experiments 1 and 2, the threshold of significance was set to $P < 0.005$ (voxel level, uncorrected). For each cluster of voxels that satisfied this criterion, the chance of finding a cluster with this or a greater size within the search volume was calculated once uncorrected (cluster-level *P*, uncorrected), and further corrected for the familywise error rate [cluster-level *P*, familywise error rate (FWER)-corrected] as implemented in SPM8. We set a threshold of 0.05 for each cluster-level analysis, and identified clusters that satisfied the FWER-corrected criterion (cluster $P < 0.05$, FWER-corrected), or those that satisfied the more liberal criterion (cluster $P < 0.05$, uncorrected). The regions of significant adaptation were further masked by a significant activation in response to the dot presentation (*t*-test, $P < 0.05$, uncorrected). For data analysis in the localiser experiments, the threshold of significance was set to $P < 0.001$ (voxel level, false discovery rate-corrected). The minimum cluster size was set to achieve the cluster-level $P < 0.05$ (uncorrected).

Results

When a red dot was presented at the same position relative to the frame in the background (Dot/Bkg), significant decreases in the BOLD signal were observed in the right precuneus (precuneus in Fig. 2A and C and Table 2; cluster-level $P = 0.030$, FWER-corrected). When a more liberal cluster-level threshold was adopted (cluster-level $P < 0.05$, uncorrected), adaptation was additionally found in the right middle occipital gyrus (MOG; Fig. 2A and Table 2). In contrast, when a dot was repeatedly presented in terms of the egocentric (eye- and head-centered) coordinates (Dot/Ego), no region showed significant adaptation in either criterion.

We also examined whether the location of the background frame was represented in the egocentric coordinates (Bkg/Ego). A few regions showed adaptation in the liberal criterion alone (Fig. 2B and D; Table 3, cluster-level $P < 0.05$, uncorrected). The largest region in the right superior parietal lobule (SPL; cool colors in Fig. 2D) was adjacent to, but mostly separated from, the precuneus region implicated for representing the dot position relative to the background (hot colors in Fig. 2C).

In our previous psychophysical study, a target location was instantaneously and automatically encoded when a background

frame was large, but the effect disappeared when the size of the frame was reduced to the size of the target (Uchimura & Kitazawa, 2013). In Experiment 2, to examine whether the brain automatically represents a dot location relative to a small frame we reduced the size of the frame to the size of the dot (Fig. 3A); thus, the small frame should serve as a landmark object rather than a background. Under this condition, no region showed adaptation in either criterion as long as the dot was presented repeatedly at the same location relative to the small frame. In contrast, significant adaptation was observed in the right SPL for repeated presentations of the dot in terms of the egocentric coordinates (Dot/Ego; Fig. 3B and Table 4; cluster-level $P = 0.035$, FWER-corrected). Notably, this SPL region (Dot/Ego; cool colors in Fig. 3C) was mostly separated from the precuneus region that was implicated as representing the dot position relative to the background (outlined with red lines in Fig. 3C, Dot/Bkg; 18 voxels of overlap out of 195 voxels, 9.3%), but the region overlapped substantially with the SPL region identified as representing the frame position in the egocentric coordinate (Bkg/Ego; Fig. 2D; 46/82, 56%). The results obtained in Experiments 1 and 2 suggest that the right precuneus region is used for representing the position of the red dot in the background coordinate automatically and that the region for the background coordinate is distinct from the right SPL region that represented the red dot (Dot/Ego) or the background frame (Bkg/Ego) in the egocentric coordinates.

We further localised the neural correlates of the background coordinate (hot colors from Experiment 1, Dot/Bkg) and the egocentric coordinate (cool colors from Experiment 2, Dot/Ego) to the areas activated by a complex sequence of opponent finger movements (Fig. 4A) and by visual stimuli flickered at 4 Hz (Fig. 4B, C and D). The right precuneus region (hot colors) was connected with the mediadorsal end of the finger movement network ($x = 11, 19$; Fig. 4A), but mostly spared from the finger movement activations. Human parietal grasp regions (hPGR, Konen *et al.*, 2013) as reported in previous literature (#11–15 in Fig. 4A; Culham *et al.*, 2003; Cavina-Pratesi *et al.*, 2007; Kroliczak *et al.*, 2007; Cavina-Pratesi *et al.*, 2010; Monaco *et al.*, 2011; Konen *et al.*, 2013), which unsurprisingly fell in or close to the finger movement network, were separated from the precuneus region by 30–40 mm in the lateral and anterior direction. Human parietal reach regions (hPRR, #1–10 in Fig. 4A; Astafiev *et al.*, 2003; Medendorp *et al.*, 2003; Prado *et al.*, 2005; Filimon *et al.*, 2009; Luaute *et al.*, 2009; Vesia *et al.*, 2010; Monaco *et al.*, 2011) were also separate from the peak by 15 mm, with the exception of the one located in the medial surface in the precuneus (#1, Astafiev *et al.*, 2003). Some hPRRs located in the superior parieto-occipital cortex (#4 and 5, Prado *et al.*, 2005; Monaco *et al.*, 2011) and the posterior parietal cortex (#7, Medendorp *et al.*, 2003) were closer to the lateral cool-colored region in the SPL ($x = 19, 28$) which represents the background or the dot in terms of the egocentric coordinates. Notably, the human homolog of the V6A (#21, Pitzalis *et al.*, 2013), which has been implicated in reaching, was located caudal to the precuneus region and closer to the egocentric region (blue color). Probably the strong involvement of the SPL in reaching movements could be related to the involvement of this area in coding the target as well as background information in egocentric coordinates.

Discussion

The current study revealed that the precuneus in the right hemisphere is involved in the automatic representation of the position

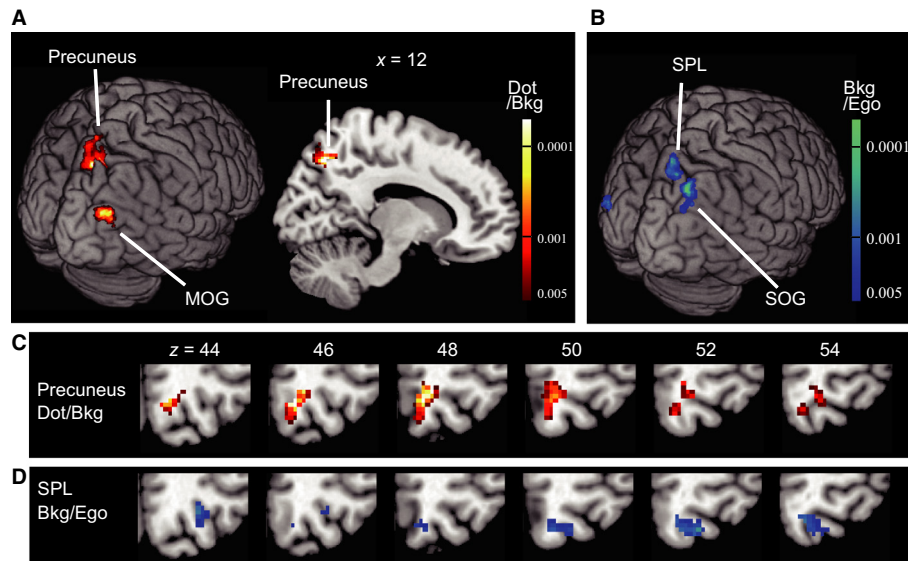


FIG. 2. Neural correlates of the dot position in the background coordinate (Experiment 1). (A) Brain regions (precuneus and the MOG) with significant adaptation (voxel level $P < 0.005$, uncorrected; cluster-level $P < 0.05$, uncorrected) as a result of repeated presentations of the dot in terms of the background frame (Dot/Bkg). The contrast used was: (novel Dot/Bkg and novel Dot/Ego + novel Dot/Bkg and repeated Dot/Ego) – (repeated Dot/Bkg and novel Dot/Ego + repeated Dot/Bkg and repeated Dot/Ego). Adaptation in the right precuneus was significant after correction for the FWER (cluster-level $P = 0.030$, FWER-corrected). (B) Brain regions (superior parietal lobule, SPL; superior occipital gyrus, SOG) with significant adaptation (voxel-level $P < 0.005$, uncorrected; cluster-level $P < 0.05$, uncorrected) as a result of repeated presentations of a frame in terms of the egocentric coordinates (Bkg/Ego). The contrast used was: novel Bkg/Ego – repeated Bkg/Ego. (C and D) Comparison of the right precuneus region (hot color in c) and the SPL region (cool color in d) mapped on sequential axial slices. Note that there is little overlap between the two.

of a visual stimulus (a red dot) in a background coordinate (Experiment 1). In contrast, no regions showed adaptation after repeated presentations of the visual stimulus in terms of the egocentric coordinates when there was the large background frame (Experiment 1). Conversely, when the size of the frame was reduced to the size of the visual stimulus (Experiment 2), the visual stimulus was no longer represented in terms of the small rectangle but was

instead represented in terms of the egocentric coordinates in a different network that involved the SPL, a major part (~90%) of which did not overlap with the precuneus allocentric region. Notably, the SEF, which has been implicated in representing a target position intentionally relative to an object both in monkeys (Olson & Gettner, 1995) and in human participants (Szczepanski *et al.*, 2013), did not show adaptation. These results show that the right

TABLE 2. Brain regions that showed significant adaptation as a result of repeated presentations of a red dot in the background frame coordinate (Experiment 1, Dot/Bkg)

AnatomicalRegion	Laterality	MNI coordinates					Cluster size	Cluster-level P	
		x	y	z	t	z		Uncorrected	FWER-corrected
Precuneus	R	12	-66	48	5.58	4.15	195	0.00037	0.030
MOG	R	40	-84	26	4.76	3.74	76	0.015	0.70

Voxels were initially thresholded at $P < 0.005$, uncorrected. The minimum cluster size was set to 46 voxels (cluster-level $P < 0.05$, uncorrected, 1 voxel = $2 \times 2 \times 2 \text{ mm}^3$). The cluster in the right precuneus was significant after correcting for the FWER.

TABLE 3. Brain regions that showed significant adaptation as a result of repeated presentations of a background frame in the egocentric (eye- and head-centered) coordinates (Experiment 1, Bkg/Ego)

Anatomical region	Laterality	MNI coordinates					Cluster size	Cluster-level P	
		x	y	z	t	z		Uncorrected	FWER-corrected
SPL	R	12	-70	56	4.25	3.46	82	0.0094	0.56
SOG	R	28	-70	42	5.09	3.91	71	0.014	0.72
MOG	L	-38	-86	6	4.38	3.53	93	0.0063	0.42
FG	R	36	-52	-16	5.80	4.25	50	0.035	0.95

SOG, superior occipital gyrus; FG, fusiform gyrus. Significant at $P < 0.005$, uncorrected. Minimum cluster size 43 voxels (cluster-level $P < 0.05$, uncorrected). None survived after FWER correction.

TABLE 4. Brain regions that showed significant adaptation as a result of repeated presentations of a red dot in the egocentric (eye- and head-centered) coordinates (Experiment 2, Dot/Ego)

Anatomical region	Laterality	MNI coordinates			<i>t</i>	<i>z</i>	Cluster size	Cluster-level <i>P</i>	
		<i>x</i>	<i>y</i>	<i>z</i>				Uncorrected	FWER-corrected
SPL	R	16	-74	52	4.71	3.71	148	0.00032	0.035
FEF	R	40	-4	52	5.64	4.18	74	0.0062	0.50
Precuneus	R	10	-56	46	4.04	3.33	65	0.0095	0.65
SPL	L	-32	-64	58	4.28	3.48	44	0.028	0.95
IPL	R	46	-34	52	4.60	3.66	37	0.041	0.99
SOG	R	22	-68	36	4.15	3.40	35	0.046	0.99
Putamen	R	24	18	-4	5.09	3.91	37	0.041	0.99
Cerebellum	R/L	4	-42	-18	5.73	4.22	43	0.029	0.96

FEF, frontal eye field; IPL, inferior parietal lobule; SOG, superior occipital gyrus. Significant at $P < 0.005$, uncorrected. Minimum cluster size 34 voxels (cluster-level $P < 0.05$, uncorrected). The cluster in the right SPL was significant after correcting for the FWER.

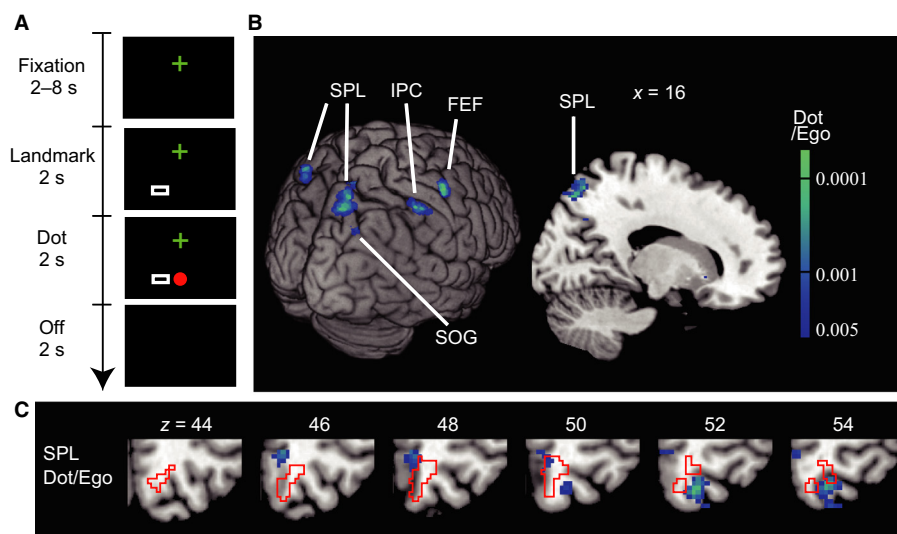


FIG. 3. Designs and results of Experiment 2 with a small landmark. (A) A large rectangular frame in Experiment 1 was reduced to the size of the dot (a small rectangle – Landmark) in Experiment 2. The conditions were otherwise the same as in Experiment 1 (Fig. 1A). (B) Regions with significant adaptation (voxel-level $P < 0.005$, uncorrected; cluster-level $P < 0.05$, uncorrected) as a result of repeated presentation of the dot, in terms of the egocentric (eye- and head-centered) coordinates (Dot/Ego). Adaptation in the right SPL was significant after correction for the FWER (cluster-level $P = 0.035$, FWER-corrected). FEF, frontal eye field; IPC, inferior parietal cortex. (C) The right SPL region superimposed on sequential axial slices. The precuneus region found in Experiment 1 is shown by red lines. Note that there is little overlap between the two.

ventral precuneus region automatically represents a stimulus position relative to the background and that the region is distinct from those representing egocentric coordinates, as in the SPL, or those representing a target position relative to an object for an endeavor, as in the SEF. Boi *et al.* (2011) reported that exogenous attention drawn by a dot can be represented relative to a background. It is thus possible that the right precuneus represents a spatial position of exogenous attention relative to the background.

The right precuneus region was generally separated from the human parietal reach or grasp regions (Konen *et al.*, 2013), as shown in Fig. 4A (hPRR, #1–10; hPGR, #11–15). Conversely, the right precuneus has been implicated in visuospatial cognitive tasks (Suchan *et al.*, 2002; Knauff *et al.*, 2003; Cavanna & Trimble, 2006) (#16 in Fig. 4A (Suchan *et al.*, 2002); #17 (Knauff *et al.*, 2003)). In addition, damage that involves the precuneus and the posterior cingulate produces a condition known as Balint's syndrome (Hécaen & Ajuriaguerra, 1954), 'the cardinal feature of which is the inability to perceive the visual field as a whole, despite intact visual fields, during simple confrontation with single small stimuli' (Raichle *et al.*, 2001). In agreement

with this, a recent study reported that the right precuneus contributed to memorising small alphabets only when they were presented in the bilateral visual fields (Kraft *et al.*, 2015). The ventral precuneus has thus been posited as 'a tonically active region of the brain that may continuously gather information about the world around' (Raichle *et al.*, 2001). The statement is nearly identical to the conclusion of the current study that the right precuneus region automatically represents a visual stimulus relative to the background.

The right precuneus region could have nothing to do with the background coordinate, but it could simply represent a flag-like shape as a whole; however, we think that this explanation is unlikely for three reasons. First, we avoided presenting the frame and the dot at once, by showing the background first for 2 s before presenting a dot at one of three positions. Second, the manipulation seems to have worked because no adaptation was observed in response to the dot presentation in the lateral occipital cortex or the posterior fusiform gyrus, which show adaptation to repeated presentations of the same shape (Kim *et al.*, 2009). Third, the precuneus region has never been implicated in object shape perception *per se*.

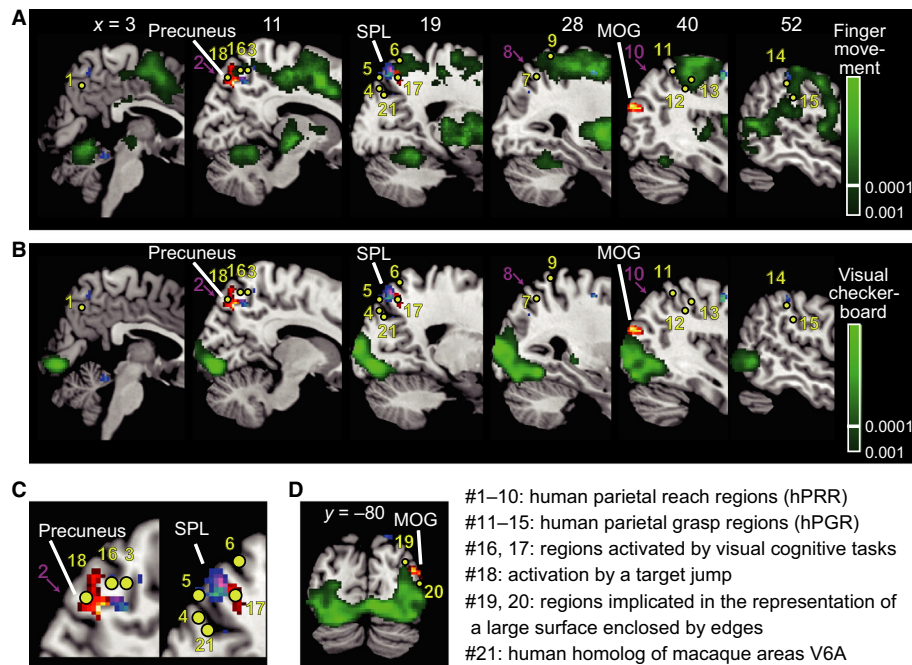


FIG. 4. Comparison of Dot/Bkg clusters in Experiment 1 (hot color, precuneus, MOG) and Dot/Ego clusters in Experiment 2 (cool color, SPL) with regions (indicated by green) significantly activated by (A) sequential opponent finger movements and by (B–D) visual stimuli (checker board patterns) flickered at 4 Hz. The green voxels were thresholded at $P < 0.001$ (voxel-level, false discovery rate-corrected). Twenty-one previously reported MNI coordinates are superimposed. Yellow dots indicate the peak activations as a result of motor, visual and cognitive tasks, and magenta arrows indicate transcranial magnetic stimulations that resulted in errors in reaching movements. See Table 5 for detail of the previous studies. (C) Magnified images of two panels in (B), $x = 11$ and 19. (D) A coronal section at $y = 80$.

TABLE 5. A list of MNI coordinates of activation reported in previous literature

No.	Reference	MNI coordinates			Tasks
		x	y	z	
1	Astafiev <i>et al.</i> (2003)	3	-63	49	Reaching
2	Vesia <i>et al.</i> (2010)	13	-80	52	Reaching
3	Filimon <i>et al.</i> (2009)	11	-54	58	Reaching
4	Monaco <i>et al.</i> (2011)	18	-79	42	Reaching
5	Prado <i>et al.</i> (2005)	19	-78	51	Reaching
6	Luaute <i>et al.</i> (2009)	18	-62	64	Reaching
7	Medendorp <i>et al.</i> (2003)	26	-62	50	Reaching
8	Vesia <i>et al.</i> (2010)	28	-60	47	Reaching
9	Prado <i>et al.</i> (2005)	28	-48	69	Reaching
10	Vesia <i>et al.</i> (2010)	41	-69	50	Reaching
11	Culham <i>et al.</i> (2003)	45	-46	55	Grasping
12	Cavina-Pratesi <i>et al.</i> (2007)	44	-36	41	Grasping
13	Monaco <i>et al.</i> (2011)	46	-31	47	Grasping
14	Kroliczak <i>et al.</i> (2007)	48	-33	45	Grasping
15	Cavina-Pratesi <i>et al.</i> (2007)	57	-26	34	Grasping
16	Suchan <i>et al.</i> (2002)	8	-59	58	Mental rotation
17	Knauff <i>et al.</i> (2003)	18	-63	52	Deductive reasoning
18	Diedrichsen <i>et al.</i> (2005)	11	-72	52	Reaching with target jump
19	Perna <i>et al.</i> (2005)	35	-83	31	Viewing an illusory surface
20	Perna <i>et al.</i> (2005)	48	-81	15	Viewing an illusory surface
21	Pitzalis <i>et al.</i> (2013)	16	-76	39	Viewing wide-field stimulation and pointing to a peripheral target

The numbers (1 to 21) correspond to those of the 21 points shown in Fig. 4.

We therefore think it probable that the significant adaptation in the right precuneus region derived from presenting the dot at the same location relative to the background, but not due to presenting the same flag-like shape as a whole.

Representation in the egocentric coordinates

The red dot was represented in the background coordinate but not in the egocentric coordinates in Experiment 1, when there was a large background frame. In contrast, when the size of the frame was reduced to the size of the visual stimulus (Experiment 2), the visual stimulus was no longer represented relative to the small rectangle but was represented in the egocentric coordinates in the right SPL. These results suggest that our brain predominantly uses the background coordinate when there are large backgrounds (as in Experiment 1) but switches to the egocentric coordinate when there is no large background (as in Experiment 2). Further, the same SPL region showed adaptation in Experiment 1 (though with the liberal criterion of cluster-level $P < 0.05$, uncorrected) after the repeated presentation of the large frame in the egocentric coordinates. These results further suggest that the egocentric region in the SPL is always at work, regardless of whether there is a background; the region is used to represent a background when there is a background and to represent a visual stimulus itself when there is no large background.

Implication of the background coordinates for error detection and visual stability

The merit of using the background to detect a target movement (target error) is worth emphasising, particularly when the eyes

move. A traditional efference copy theory assumes that the efference copy of the eye movement is used to estimate the future retinal position of the target, and the prediction is compared with the actual outcome (Medendorp, 2011; Golomb & Kanwisher, 2012). In contrast, a target's movement can be detected by representing the target relative to the background without paying attention to the eye movements *per se*. In fact, the detection of a target object displacement during a saccade is made in relation to other landmarks in the scene (Deubel, 2004; Germeys *et al.*, 2004). In addition, a previous functional imaging study (Diedrichsen *et al.*, 2005) reported that a target error in reaching movements, induced by a target jump during the movement, was represented in the right precuneus, which fell within the precuneus region in the current study (#18 in Fig. 4A). It is reasonable that the error resulting from the target jump is represented in the right precuneus region, which is now implicated in the representation of the background coordinate.

Extending this line further, we speculate that the background coordinate in the right precuneus contributes not only to maintaining spatial constancy of a movement goal but also to maintaining visual stability across saccadic eye movements. This original view may provide a solution to the long-lasting debate on how and why the external world remains stable while we move our eyes (Bays & Husain, 2007; Wurtz, 2008; Melcher, 2011). The relationship between automatic neural representations of visual objects in the background frame coordinate in the right precuneus and our visual awareness of stability merits further investigation.

Acknowledgements

The study was supported by Grants-in-Aid for Scientific Research on Innovative Areas 25119002 to S.K., 251195040 to T.N., and (A) 25240022 to S.K., a Health Labour Sciences Research Grant from the Ministry of Health Labour and Welfare to S.K. and a Japan Society for the Promotion of Science Research Fellowships for Young Scientists award to M.U. The authors declare no competing financial interests.

Abbreviations

Bkg, background; Ego, egocentric (eye- and head-centered); FWER, family-wise error rate; hPGR, human parietal grasp region; hPRR, human parietal reach region; MOG, middle occipital gyrus; SEF, supplementary eye field; SPL, superior parietal lobule.

References

Astafiev, S.V., Shulman, G.L., Stanley, C.M., Snyder, A.Z., Van Essen, D.C. & Corbetta, M. (2003) Functional organization of human intraparietal and frontal cortex for attending, looking, and pointing. *J. Neurosci.*, **23**, 4689–4699.

Baloh, R.W., Sills, A.W., Kumley, W.E. & Honrubia, V. (1975) Quantitative measurement of saccade amplitude, duration, and velocity. *Neurology*, **25**, 1065–1070.

Bays, P.M. & Husain, M. (2007) Spatial remapping of the visual world across saccades. *NeuroReport*, **18**, 1207–1213.

Bernier, P.M. & Grafton, S.T. (2010) Human posterior parietal cortex flexibly determines reference frames for reaching based on sensory context. *Neuron*, **68**, 776–788.

Blankenburg, F., Ruben, J., Meyer, R., Schwieemann, J. & Villringer, A. (2003) Evidence for a rostral-to-caudal somatotopic organization in human primary somatosensory cortex with mirror-reversal in areas 3b and 1. *Cereb. Cortex*, **13**, 987–993.

Boi, M., Vergeer, M., Ogmen, H. & Herzog, M.H. (2011) Nonretinotopic exogenous attention. *Curr. Biol.*, **21**, 1732–1737.

Byrne, P.A., Cappadocia, D.C. & Crawford, J.D. (2010) Interactions between gaze-centered and allocentric representations of reach target location in the presence of spatial updating. *Vision Res.*, **50**, 2661–2670.

Cavanna, A.E. & Trimble, M.R. (2006) The precuneus: a review of its functional anatomy and behavioural correlates. *Brain*, **129**, 564–583.

Cavina-Pratesi, C., Goodale, M.A. & Culham, J.C. (2007) fMRI reveals a dissociation between grasping and perceiving the size of real 3D objects. *PLoS One*, **2**, e424.

Cavina-Pratesi, C., Monaco, S., Fattori, P., Galletti, C., McAdam, T.D., Quinlan, D.J., Goodale, M.A. & Culham, J.C. (2010) Functional magnetic resonance imaging reveals the neural substrates of arm transport and grip formation in reach-to-grasp actions in humans. *J. Neurosci.*, **30**, 10306–10323.

Chafee, M.V., Averbeck, B.B. & Crowe, D.A. (2007) Representing spatial relationships in posterior parietal cortex: single neurons code object-referenced position. *Cereb. Cortex*, **17**, 2914–2932.

Crespi, S., Biagi, L., d'Avossa, G., Burr, D.C., Tosetti, M. & Morrone, M.C. (2011) Spatiotopic coding of BOLD signal in human visual cortex depends on spatial attention. *PLoS One*, **6**, e21661.

Culham, J.C., Danckert, S.L., DeSouza, J.F.X., Gati, J.S., Menon, R.S. & Goodale, M.A. (2003) Visually guided grasping produces fMRI activation in dorsal but not ventral stream brain areas. *Exp. Brain Res.*, **153**, 180–189.

d'Avossa, G., Tosetti, M., Crespi, S., Biagi, L., Burr, D.C. & Morrone, M.C. (2007) Spatiotopic selectivity of BOLD responses to visual motion in human area MT. *Nat. Neurosci.*, **10**, 249–255.

Deubel, H. (2004) Localization of targets across saccades: role of landmark objects. *Vis. Cogn.*, **11**, 173–202.

Diedrichsen, J., Hashambhoy, Y., Rane, T. & Shadmehr, R. (2005) Neural correlates of reach errors. *J. Neurosci.*, **25**, 9919–9931.

Duhamel, J.R., Bremner, F., Ben Hamed, S. & Graf, W. (1997) Spatial invariance of visual receptive fields in parietal cortex neurons. *Nature*, **389**, 845–848.

Filimon, F., Nelson, J.D., Huang, R.S. & Sereno, M.I. (2009) Multiple parietal reach regions in humans: cortical representations for visual and proprioceptive feedback during on-line reaching. *J. Neurosci.*, **29**, 2961–2971.

Galletti, C., Battaglini, P.P. & Fattori, P. (1993) Parietal neurons encoding spatial locations in craniotopic coordinates. *Exp. Brain Res.*, **96**, 221–229.

Germeys, F., de Graef, P., Panis, S., van Eccelpoel, C. & Verfaillie, K. (2004) Transsaccadic integration of bystander locations. *Vis. Cogn.*, **11**, 203–234.

Golomb, J.D. & Kanwisher, N. (2012) Retinotopic memory is more precise than spatiotopic memory. *Proc. Natl. Acad. Sci. USA*, **109**, 1796–1801.

Grill-Spector, K., Henson, R. & Martin, A. (2006) Repetition and the brain: neural models of stimulus-specific effects. *Trends Cogn. Sci.*, **10**, 14–23.

Hécaen, H. & Ajuriaguerra, J. (1954) Balint's syndrome (psychic paralysis of visual fixation) and its minor forms. *Brain*, **77**, 373–400.

Kansaku, K., Muraki, S., Umeyama, S., Nishimori, Y., Kochiyama, T., Yamane, S. & Kitazawa, S. (2005) Cortical activity in multiple motor areas during sequential finger movements: an application of independent component analysis. *NeuroImage*, **28**, 669–681.

Karn, K.S., Moller, P. & Hayhoe, M.M. (1997) Reference frames in saccadic targeting. *Exp. Brain Res.*, **115**, 267–282.

Kim, J.G., Biederman, I., Lescroart, M.D. & Hayworth, K.J. (2009) Adaptation to objects in the lateral occipital complex (LOC): shape or semantics? *Vision Res.*, **49**, 2297–2305.

Knauff, M., Fangmeier, T., Ruff, C.C. & Johnson-Laird, P.N. (2003) Reasoning, models, and images: behavioral measures and cortical activity. *J. Cognitive Neurosci.*, **15**, 559–573.

Konen, C.S., Mruczek, R.E., Montoya, J.L. & Kastner, S. (2013) Functional organization of human posterior parietal cortex: grasping- and reaching-related activations relative to topographically organized cortex. *J. Neurophysiol.*, **109**, 2897–2908.

Kraft, A., Dyrholm, M., Kehler, S., Kaufmann, C., Bruening, J., Kathmann, N., Bundesen, C., Irlbacher, K. & Brandt, S.A. (2015) TMS over the right precuneus reduces the bilateral field advantage in visual short term memory capacity. *Brain Stimul.*, **8**, 216–223.

Kroliczak, G., Cavina-Pratesi, C., Goodman, D.A. & Culham, J.C. (2007) What does the brain do when you fake it? An fMRI study of pantomimed and real grasping. *J. Neurophysiol.*, **97**, 2410–2422.

Lin, Z. & He, S. (2012) Automatic frame-centered object representation and integration revealed by iconic memory, visual priming, and backward masking. *J. Vision*, **12**, 1–18.

Luaute, J., Schwartz, S., Rossetti, Y., Spiridon, M., Rode, G., Boisson, D. & Vuilleumier, P. (2009) Dynamic changes in brain activity during prism adaptation. *J. Neurosci.*, **29**, 169–178.

- Martinez-Conde, S., Macknik, S.L., Troncoso, X.G. & Hubel, D.H. (2009) Microsaccades: a neurophysiological analysis. *Trends Neurosci.*, **32**, 463–475.
- McKyton, A. & Zohary, E. (2007) Beyond retinotopic mapping: the spatial representation of objects in the human lateral occipital complex. *Cereb. Cortex*, **17**, 1164–1172.
- Medendorp, W.P. (2011) Spatial constancy mechanisms in motor control. *Philos. T. Roy. Soc. B.*, **366**, 476–491.
- Medendorp, W.P., Goltz, H.C., Vilis, T. & Crawford, J.D. (2003) Gaze-centered updating of visual space in human parietal cortex. *J. Neurosci.*, **23**, 6209–6214.
- Melcher, D. (2011) Visual stability. *Philos. T. Roy. Soc. B.*, **366**, 468–475.
- Monaco, S., Cavina-Pratesi, C., Sedda, A., Fattori, P., Galletti, C. & Culham, J.C. (2011) Functional magnetic resonance adaptation reveals the involvement of the dorsomedial stream in hand orientation for grasping. *J. Neurophysiol.*, **106**, 2248–2263.
- Nakano, T., Kato, M., Morito, Y., Itoi, S. & Kitazawa, S. (2013) Blink-related momentary activation of the default mode network while viewing videos. *Proc. Natl. Acad. Sci. USA*, **110**, 702–706.
- Obhi, S.S. & Goodale, M.A. (2005) The effects of landmarks on the performance of delayed and real-time pointing movements. *Exp. Brain Res.*, **167**, 335–344.
- Oldfield, R.C. (1971) The assessment and analysis of handedness: the Edinburgh inventory. *Neuropsychologia*, **9**, 97–113.
- Olson, C.R. & Gettner, S.N. (1995) Object-centered direction selectivity in the macaque supplementary eye field. *Science*, **269**, 985–988.
- Perna, A., Tosetti, M., Montanaro, D. & Morrone, M.C. (2005) Neuronal mechanisms for illusory brightness perception in humans. *Neuron*, **47**, 645–651.
- Pitzalis, S., Sereno, M.I., Committeri, G., Fattori, P., Galati, G., Tsoni, A. & Galletti, C. (2013) The human homologue of macaque area V6A. *NeuroImage*, **82**, 517–530.
- Prado, J., Clavagnier, S., Otzenberger, H., Scheiber, C., Kennedy, H. & Perenin, M.T. (2005) Two cortical systems for reaching in central and peripheral vision. *Neuron*, **48**, 849–858.
- Raichle, M.E., MacLeod, A.M., Snyder, A.Z., Powers, W.J., Gusnard, D.A. & Shulman, G.L. (2001) A default mode of brain function. *Proc. Natl. Acad. Sci. USA*, **98**, 676–682.
- Sereno, M.I., Dale, A.M., Reppas, J.B., Kwong, K.K., Belliveau, J.W., Brady, T.J., Rosen, B.R. & Tootell, R.B. (1995) Borders of multiple visual areas in humans revealed by functional magnetic resonance imaging. *Science*, **268**, 889–893.
- Sereno, M.I. & Huang, R.S. (2006) A human parietal face area contains aligned head-centered visual and tactile maps. *Nat. Neurosci.*, **9**, 1337–1343.
- Sheth, B.R. & Shimojo, S. (2004) Extrinsic cues suppress the encoding of intrinsic cues. *J. Cognitive Neurosci.*, **16**, 339–350.
- Suchan, B., Yaguez, L., Wunderlich, G., Canavan, A.G., Herzog, H., Tellmann, L., Homberg, V. & Seitz, R.J. (2002) Hemispheric dissociation of visual-pattern processing and visual rotation. *Behav. Brain Res.*, **136**, 533–544.
- Szczepanski, S.M., Pinsk, M.A., Douglas, M.M., Kastner, S. & Saalmann, Y.B. (2013) Functional and structural architecture of the human dorsal frontoparietal attention network. *Proc. Natl. Acad. Sci. USA*, **110**, 15806–15811.
- Uchimura, M. & Kitazawa, S. (2013) Cancelling prism adaptation by a shift of background: a novel utility of allocentric coordinates for extracting motor errors. *J. Neurosci.*, **33**, 7595–7602.
- Van Pelt, S., Toni, I., Diedrichsen, J. & Medendorp, W.P. (2010) Repetition suppression dissociates spatial frames of reference in human saccade generation. *J. Neurophysiol.*, **104**, 1239–1248.
- Vesia, M., Prime, S.L., Yan, X., Sergio, L.E. & Crawford, J.D. (2010) Specificity of human parietal saccade and reach regions during transcranial magnetic stimulation. *J. Neurosci.*, **30**, 13053–13065.
- Weibull, A., Bjorkman, A., Hall, H., Rosen, B., Lundborg, G. & Svensson, J. (2008) Optimizing the mapping of finger areas in primary somatosensory cortex using functional MRI. *Magn. Reson. Imaging*, **26**, 1342–1351.
- Wurtz, R.H. (2008) Neuronal mechanisms of visual stability. *Vision Res.*, **48**, 2070–2089.